Journal of Power Sources 242 (2013) 244–254

Contents lists available at SciVerse ScienceDirect

Journal of Power Sources

journal homepage: www.elsevier.com/locate/jpowsour

In situ measurement of active catalyst surface area in fuel cell stacks

E. Brightman [a,*], G. Hinds [a], R. O'Malley [b]

[a] National Physical Laboratory, Teddington, Middlesex TW11 0LW, United Kingdom
[b] Johnson Matthey Fuel Cells, Lydiard Fields, Great Western Way, Swindon, Wiltshire SN5 8AT, United Kingdom

HIGHLIGHTS

- Novel in situ technique for measuring active surface area in PEMFC stacks.
- Simultaneous measurement of every cell in an 18-cell stack demonstrated.
- Invaluable tool for state of health monitoring during fuel cell durability tests.

ARTICLE INFO

Article history:
Received 17 December 2012
Received in revised form
16 April 2013
Accepted 9 May 2013
Available online 30 May 2013

Keywords:
In situ
Fuel cells
Electrochemical surface area
Galvanostatic measurement
PEMFC stack

ABSTRACT

Measurement of electrochemical surface area (ECSA) of fuel cell electrodes is a key diagnostic of performance and gives a useful parameter for monitoring degradation and state of health in polymer electrolyte membrane fuel cells (PEMFCs). However, conventional methods for determining ECSA require potentiostatic control of the cell, which is impractical in a fuel cell stack. Here we demonstrate for the first time the practical application of a galvanostatic technique that enables in situ monitoring of ECSA in each cell throughout the lifetime of a stack. The concept is demonstrated at single cell level using both H adsorption and CO stripping, and the H adsorption (cathodic current) method is extended to stack testing. The undesirable effects of H_2 crossover on the measurement may be minimised by appropriate selection of current density and by working with dilute H_2 on the anode electrode. Good agreement is achieved with ECSA values determined using conventional single cell voltammetry across a range of MEA designs. The technique is straightforward to implement and provides an invaluable tool for state of health monitoring during PEMFC stack lifetime studies.

1. Introduction

One of the main challenges for the successful commercialisation of polymer electrolyte membrane fuel cells (PEMFCs) is the optimisation of catalyst utilisation, in order to minimise the amount of platinum required. The catalyst layer is typically formed of small particles of polycrystalline platinum or platinum-alloy dispersed on a high surface area support such as carbon black. This helps to maximise the number of catalytically active sites per gram of platinum used and means that the catalytic surface area of a fuel cell electrode is very much higher than the geometrical electrode area. In a PEMFC, not all the platinum is electrochemically active due to discontinuities in the electronic, ionic and gas phases, and the degradation of the electrode over time due to agglomeration and loss of platinum particles is associated with a concomitant decrease in electrochemical surface area (ECSA) [1]. The ECSA of an electrode is therefore an important performance metric that provides an estimate of catalyst utilisation and degradation.

In order to make valid measurements of critical parameters that are applicable to commercial cell and stack hardware, in situ techniques must be developed. Until recently, the ECSA of PEMFC electrodes has only been studied ex situ in aqueous electrolytes, or in single cell configurations. The standard technique for determining ECSA in a single cell is by measurement of the charge associated with the oxidation or reduction of a monolayer of adsorbed species, typically either hydrogen or carbon monoxide (CO) [2,3]. In both these cases, the measurement is made using cyclic voltammetry (CV) with the electrode of interest acting as the working electrode, supplied with an inert gas such as N_2, and the counter electrode supplied with H_2 functioning as a pseudo-reference electrode.

In the method using hydrogen desorption/adsorption, protons present in the electrolyte are reduced to form a monolayer of electro-adsorbed hydrogen on the platinum surface (Eq. (1)). The Pt-H species formed, so-called underpotential deposited hydrogen (H_{upd}), is distinct from the intermediate involved in the hydrogen

* Corresponding author. Tel.: +44 (0)20 8943 8564; fax: +44 (0)20 8943 6458.
E-mail address: edward.brightman@npl.co.uk (E. Brightman).

0378-7753/$ – see front matter
http://dx.doi.org/10.1016/j.jpowsour.2013.05.046

evolution reaction, which is driven by application of an overpotential. A detailed explanation of this mechanism is given by Conway and Jerkiewicz [4].

$$Pt_{(surface)} + H_3O^+ + e^- \rightleftharpoons Pt - H_{upd} + H_2O \quad (1)$$

The reaction in Eq. (1) involves a range of adsorption energies due to the polycrystalline nature of the platinum catalyst and so the potential at which this occurs ranges from 0.05 to 0.40 V vs. the standard hydrogen electrode (SHE) [2]. The measurement of ECSA by this method is based on the assumption that each proton is able to occupy one site on the available platinum surface, and that all sites that are active and accessible are occupied during the measurement.

In the CO oxidative desorption method, the platinum catalyst under investigation is exposed to CO, which chemisorbs strongly in a monolayer on the platinum surface. The electrode is then switched to an inert gas supply and the potential swept up to oxidising potentials, showing a sharp peak in current corresponding to oxidation of CO at around 0.7 V vs. SHE.

In both methods the surface area is estimated using a conversion factor determined from smooth crystalline platinum surfaces, which is known to be about 210 $\mu C\ cm^{-2}$ for H adsorption [5]. In the case of CO stripping, the charge associated with the oxidation peak of CO is generally assumed to be equivalent to two electrons per CO molecule, and so the conversion factor is assumed to be double that for H adsorption, i.e. ~420 $\mu C\ cm^{-2}$ [3]. The ECSA of the electrode in units of $m^2\ g^{-1}$ is then calculated using the following formula:

$$ECSA = \frac{Q}{\Gamma L} \quad (2)$$

where Q is the integrated charge density ($C\ cm^{-2}$), Γ is the specific charge required to oxidise/reduce a monolayer of the adsorbed species (i.e. 210 or 420 × $\mu C\ cm^{-2}$), and L is the platinum loading of the electrode ($g\ m^{-2}$). The technique can also be used to measure the surface area of platinum per unit geometrical area of the electrode, or roughness factor, without requiring knowledge of the platinum loading L. This value is usually given in units $cm^2_{(Pt)}\ cm^{-2}_{(electrode)}$.

Use of the conventional technique for ECSA measurement in single cells requires potentiodynamic control of the cell. This is impractical in a fuel cell stack, firstly because the potential of individual cells cannot be controlled independently due to the electrical connections between them and secondly because of the prohibitively long time required to measure the ECSA of each individual cell in sequence, particularly for large stacks. A recent publication by Wasterlain et al. has demonstrated a technique for measuring ECSA of cells in a stack by a combined CV technique, which relies on the assumption that the cells behave in a homogeneous way and that the sweep rate is uniform through the stack [6]. However, this assumption is rarely valid, particularly for stacks containing membrane electrode assemblies (MEAs) with different Pt loadings, in which case the potential difference applied to the stack will not be equally divided among the cells and there would be a risk of damaging cells by exposing them to highly oxidising potentials. Furthermore, the experiment requires specialist hardware which is not easily integrated into test systems.

Here we report on a novel galvanostatic technique for measurement of ECSA in fuel cell stacks, which has been developed independently by two separate groups: the present authors and also researchers in Korea. In their recent paper, Lee et al. [7] investigated the use of a current-controlled method to determine ECSA by applying a constant current to the cell and measuring the rate of change of the electrode potential. This gives equivalent information to a CV, as previously shown by Stevens and Dahn for ex situ Pt/C samples in aqueous electrolyte [8]. Lee et al. showed that by applying a fixed current to a PEMFC, a reliable estimate of ECSA could be obtained in situ, in a method that could be easily applied to stack assemblies.

The present work describes the results from the parallel development of this technique at the National Physical Laboratory (NPL), using both H adsorption/desorption and CO stripping, and moreover, extends the application of the method to a viable stack diagnostic procedure carried out on commercially relevant hardware at Johnson Matthey Fuel Cells (JMFC). We demonstrate an easily-implemented test procedure taking steps to minimise the impact of hydrogen crossover, and investigate the sensitivity of the technique to electrode loading, membrane permeability, and degradation.

2. Experimental

2.1. Single cell tests

2.1.1. Test setup

The single cell tests were performed on MEAs supplied by JMFC (Pt/C anode/cathode, perfluorosulfonic acid (PFSA) membrane), using a Greenlight FCATS-G50 fuel cell test stand. The test stand was used for gas flow control and humidification, while a separate Gill AC potentiostat (ACM Instruments Ltd.) was used to perform the voltammetric/potentiometric measurements. The reference and counter electrode connectors of the potentiostat were attached to the anode current collector of the fuel cell, while the working electrode was connected to the cathode current collector of the fuel cell. (N.B. For simplicity, the fuel cell cathode and fuel cell anode are nominally referred to as “cathode” and “anode” throughout, even though in certain measurements either anodic or cathodic processes may be occurring at these electrodes.) Three-way switching valves were fitted to facilitate switching of the cathode gas supply between air, N_2 and 1% CO in N_2.

All measurements were carried out at room temperature and atmospheric pressure. For the H desorption/adsorption experiments, the fuel cell cathode was supplied with humidified nitrogen (100% relative humidity (RH)) at a flow rate of 0.5 standard litres per minute (SLPM), while the anode was supplied with humidified hydrogen (100% RH) at a flow rate of 0.5 SLPM and functioned as a reversible hydrogen electrode. The cell was allowed to equilibrate before commencing the voltammetry tests, during which time hydrogen diffusing through the membrane adsorbed on the cathode catalyst surface, resulting in a steady state potential of ~0.1 V. The importance of this hydrogen crossover rate on the measurements will be discussed further in due course.

For the CO stripping tests, hydrogen was again supplied to the anode at a constant flow rate of 0.5 SLPM. The cathode was exposed to 1% CO in N_2 (BOC Special Gases Ltd, UK) flowing at 0.5 SLPM for approximately 15–20 min. Before the measurements were made, the gas supply was switched to pure N_2 at the same flow rate until the cell potential was steady, which took around 20 min.

In all experiments, the fuel cell anode was used as a pseudo-reference electrode (assumed to be 0.0 V vs SHE), and potentials are quoted with respect to this.

2.1.2. Cyclic voltammetry

The MEAs were characterised with a standard CV test in order to obtain a benchmark value of the ECSA for comparison with the galvanostatic method. For the measurement using H adsorption/desorption, the cell potential was swept at 10 $mV\ s^{-1}$ between 0.05 V and 0.80 V. For cyclic voltammetry experiments using CO stripping, the potential was swept between 0.05 V and 1.2 V at 5, 10

and 20 mV s^{-1}, with 3 cycles per scan, the second and third cycles being used to provide the baseline for determining the charge associated with CO stripping.

2.1.3. Galvanostatic experiments

For the measurements under galvanostatic control the cell was prepared in the same way as for the cyclic voltammetry experiments. For H desorption/adsorption measurements, the cell was held at a fixed positive current and the cell potential was monitored with time until a potential limit of 0.8 V was reached to avoid oxidation of the carbon support at higher potentials. The current was then reversed and held constant until the potential reached a steady state. Current densities of 0.5 mA cm^{-2}, 1 mA cm^{-2}, 2 mA cm^{-2}, 4 mA cm^{-2} and 8 mA cm^{-2} were initially used, and repeat measurements were made with a maximum current density of 6 mA cm^{-2} since the charge/discharge rate was found to be too fast to resolve accurately at 8 mA cm^{-2}. For the voltage measurement, data acquisition rates in the range 1–50 Hz were used to obtain an adequate resolution depending on the current density applied. For the CO stripping measurements, the upper potential limit was set at 1.2 V, and the experiments were each repeated without CO in order to obtain a baseline voltammogram. Current densities of 0.8, 1, 2, 4 and 6 mA cm^{-2} were used, with a constant N_2 flow rate of 0.5 SLPM. The CO oxidation reaction only occurs in the anodic regime, i.e. at positive current densities. However, in the experimental procedure used, a negative current density was also applied after the cell potential had risen to 1.2 V in order to reduce any PtO that may have formed and to re-equilibrate the cell.

The potential transients obtained in the galvanostatic tests were converted to pseudo-CV form using a method developed by Stevens and Dahn for determination of ECSA on Pt/C samples in aqueous electrolyte [8]. Here numerical differentiation of the potential with respect to time is carried out to give $\Delta V/\Delta t$. This is then used to calculate differential capacity (dQ/dV) using the following relationship:

$$(dQ/dV) \approx \Delta Q/\Delta V = (I\Delta t)/(\Delta V) \quad (3)$$

where I is the galvanostatic current density. When plotted against cell potential, a pseudo-CV is obtained which can be directly compared to a conventionally measured potentiodynamic CV.

2.2. Stack tests

2.2.1. Stack design

The current-controlled ECSA method was validated in an 18-cell stack of ~200 cm^2 active area tested on a JMFC stack test stand designed and built in-house. In order to address concerns over (i) the impact of hydrogen crossover and (ii) Pt loading sensitivity, a specific series of samples was designed for technique validation work. MEAs comprising standard Pt/C electrocatalysts were fabricated with anode Pt loadings of 0.1 mg cm^{-2} and a range of cathode Pt loadings. Additionally, two differing reinforced PFSA membranes were selected that are known to exhibit very different hydrogen permeation behaviour. The hydrogen crossover current density as determined by standard electrochemical methods was approximately 1.3 mA cm^{-2} for Membrane 1 and approximately 2.5 mA cm^{-2} for Membrane 2; it should be noted that Membrane 2 was selected as a material with unusually high crossover and thus represents a 'worst-case scenario' within the context of this particular test method.

The combination of the three cathode loadings and two membranes resulted in six MEA variants which were built into an 18-cell stack in a block configuration – see Table 1. The stack was specifically designed to ensure that one of each MEA variant was (i) neighboured by equivalent samples (i.e. Cells 2, 5, 8, 11, 14, 17); and (ii) neighboured by different samples to ascertain whether there is an influence of MEA environment on the measured ECSA.

Table 1
Stack configuration.

Cell #	MEA description
1	0.35 mg_{Pt} cm^{-2}:Membrane 1
2	0.35 mg_{Pt} cm^{-2}:Membrane 1
3	0.35 mg_{Pt} cm^{-2}:Membrane 1
4	0.21 mg_{Pt} cm^{-2}:Membrane 1
5	0.21 mg_{Pt} cm^{-2}:Membrane 1
6	0.21 mg_{Pt} cm^{-2}:Membrane 1
7	0.17 mg_{Pt} cm^{-2}:Membrane 1
8	0.17 mg_{Pt} cm^{-2}:Membrane 1
9	0.19 mg_{Pt} cm^{-2}:Membrane 1
10	0.20 mg_{Pt} cm^{-2}:Membrane 2
11	0.20 mg_{Pt} cm^{-2}:Membrane 2
12	0.15 mg_{Pt} cm^{-2}:Membrane 2
13	0.18 mg_{Pt} cm^{-2}:Membrane 2
14	0.22 mg_{Pt} cm^{-2}:Membrane 2
15	0.22 mg_{Pt} cm^{-2}:Membrane 2
16	0.36 mg_{Pt} cm^{-2}:Membrane 2
17	0.36 mg_{Pt} cm^{-2}:Membrane 2
18	0.35 mg_{Pt} cm^{-2}:Membrane 2

2.2.2. Galvanostatic ECSA measurements

For the stack tests, H^+ reduction rather than H oxidation was used, i.e. a negative current was applied, such that the cell potentials drift from high to low, protecting the stack components from damage at positive potentials which might occur if using a positive current. Although a H_2 concentration of 100% is employed during typical stack operation, such high H_2 levels are not required within this particular test method in which the objective is simply to maintain a constant potential (i.e. ~0 V) at the anode. Ideally, as low an H_2 concentration as possible should be used on the anode (to minimise crossover) but without compromising the ability of the electrocatalyst layer to maintain a steady reference potential. However, in practice the ranges of the mass flow controllers on the stack test stands used in this work limited the minimum hydrogen concentration to 10%. Thus, to understand the impact of anode H_2 concentration on the measured ECSA value, testing commenced with 10% H_2 and this value was systematically increased.

The stack was conditioned overnight at 500 mA cm^{-2}, 80 °C, 100% $RH_{anode/cathode}$, 1.5:2.0 H_2:Air stoichiometry and gas inlet pressures of 100 kPag. Before voltage discharge measurements were made, the gas supply on the cathode was switched from air to N_2 and that on the anode from 100% H_2 to the desired H_2 concentration. Before the voltage of any cell dropped below 0.8 V a fixed negative current was applied to the stack using a potentiostat and the subsequent discharge voltage of each cell was recorded at 1 s intervals. The test was complete when the voltage on all cells had dropped to 0.1 V. The charge passed in forming a monolayer of adsorbed H_{upd} was then calculated from the time taken for the cell voltage to drop from 0.4 V to 0.1 V. The accuracy of this was limited by the time resolution of the stack testing equipment used, and subsequent users of this technique may not be limited in this way. The error bars in Figs. 10 and 11 reflect the calculated error introduced by this limitation, which is less than the measurement uncertainty caused by other factors. This will be discussed further in the results section.

2.2.3. Membrane aging

In order to investigate the effect of membrane degradation on the ECSA measurement, membrane aging was carried out at open circuit under dry conditions. The conditions used for this test were

13% $RH_{anode/cathode}$, 80 °C, H_2/air flows as per 200 mA cm^{-2} (1.5/2 stoichiometry) and 13 kPag anode/cathode.

3. Results and discussion

3.1. Single cell tests

3.1.1. Cyclic voltammetry

A preliminary CV test was used to provide a benchmark estimate of the ECSA for comparison with the galvanostatic data. Voltammograms for both H adsorption/desorption and CO stripping voltammetry at a sweep rate of 10 mV s^{-1} are shown in Fig. 1(a) and (b) respectively. The shaded areas correspond to the charge density associated with H adsorption/desorption and CO oxidation. The calculated ECSA values for the electrode from the CV measurements are summarised in Table 2. The CO stripping method gives slightly lower values for ECSA than those obtained with H adsorption, but with good repeatability. The lower value may be due partly to uncertainty in the extrapolation of the peak to the baseline, but it is also likely to be associated with a different kinetic mechanism for CO stripping compared to H adsorption, resulting in a smaller proportion of adsorption sites occupied by CO. No significant effect of scan rate was evident in the CO stripping measurements.

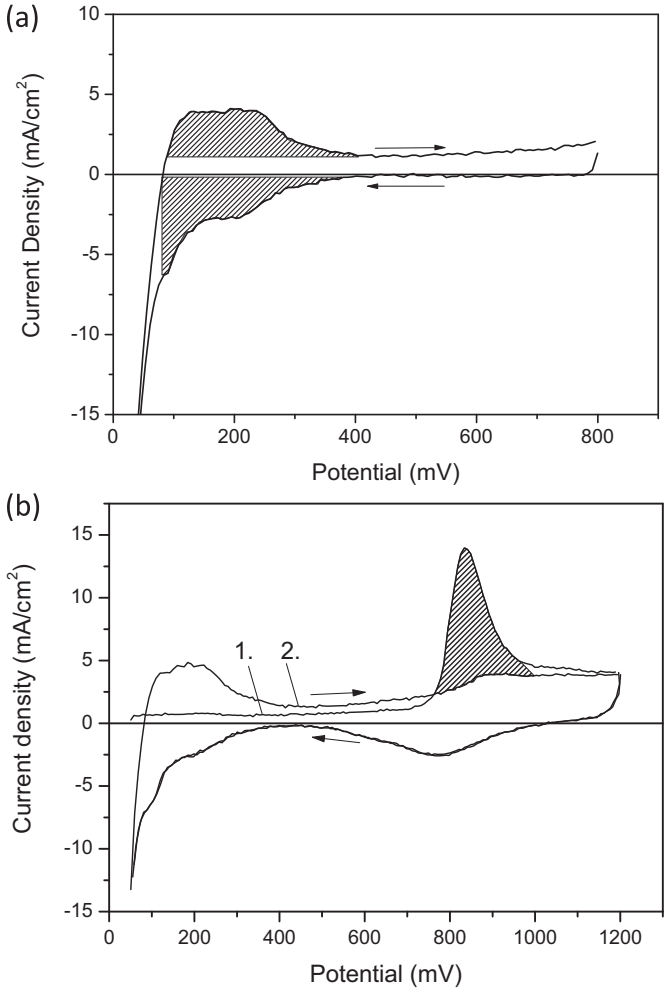

Fig. 1. (a) H adsorption CV for MEA 1. (b) CO stripping CV. Sweep 1 = CO stripping process. Sweep 2 = baseline.

Table 2
Benchmark ECSA values determined by cyclic voltammetry.

Method	Scan rate (mV s^{-1})	ECSA (m^2 g_{Pt}^{-1})
H oxidation	10	73 ± 3
H+ reduction	10	77 ± 10
CO stripping	5	63 ± 5
	10	63 ± 6
	20	60 ± 6

3.1.2. Galvanostatic tests – H adsorption method

Potential-time plots from the galvanostatic tests using H desorption/adsorption are shown as a function of current density in Fig. 2(a) and (b). The plot for the lowest current density (0.5 mA cm^{-2}) is not included in Fig. 2(a) due to the much longer time scale required for the voltage limit to be obtained. As expected, the average rate of change of potential with time increases with current density. In order to determine the charge associated with H oxidation and H^+ reduction, the shape of the curves must be analysed to interpret the subtle changes in gradient correctly. At any given fixed current a small gradient indicates the occurrence of Faradaic processes while a large gradient indicates that only double layer charging is occurring. This becomes more apparent when the potential transients are converted to pseudo-CV form according to the method described in Section 2 and the results of this are plotted in Fig. 2(c), which can now be compared to the original CV data in Fig. 1(a). Plotting the data in this way facilitates determination of the point at which hydrogen evolution begins to dominate on the cathodic sweep, as the point at which the pseudocapacitance (*y*-axis) becomes asymptotic around 100 mV. The approximate point at which this occurs has been highlighted in its equivalent position on the potential/time curves in Fig. 2(b).

In order to determine the charge density *Q* associated with H oxidation or H^+ reduction (and hence ECSA), the time taken to complete the process may simply be read from the potential/time plots in Fig. 2(a) and (b). However, this gives a result that includes contributions to the total charge passed (*Q*) from both hydrogen crossover and double layer charging. Lee et al. [7] showed that it is possible by further analysis and by using a range of current densities to separate out the contributions of hydrogen crossover and double layer charging. However, the aim of this study was to develop a method that could be applied to automated stack testing and this additional level of analysis was considered unnecessary for this purpose, provided that suitable caveats were taken into account when interpreting the data.

Using the pseudo-CV in Fig. 2(c) as a guide, the regions of interest can be approximated as the time from zero to the point of inflection on the oxidative sweep and the time from 400 mV to the onset of hydrogen evolution on the reductive sweep respectively. This time multiplied by the applied current density gives a charge density *Q*, Eq. (3), which can then be used to calculate the ECSA using Eq. (2). The results from this analysis are displayed in Table 3. When compared to the values in Table 2, the H oxidation measurements significantly overestimate the ECSA value at lower current densities due to the more significant effect of hydrogen crossover. Hydrogen permeating through the membrane must be oxidised in addition to the H_{upd} adsorbed on the Pt electrode surface, resulting in an overestimate of the apparent Pt surface area. The reductive sweep is affected in the opposite way, where adsorption of crossover hydrogen occurs in addition to reduction of H^+, giving an underestimate of Pt surface area at low, negative current densities. This effect is less pronounced than for positive currents.

The repeatability of the technique was assessed by carrying out the H adsorption experiments twice more at current densities of

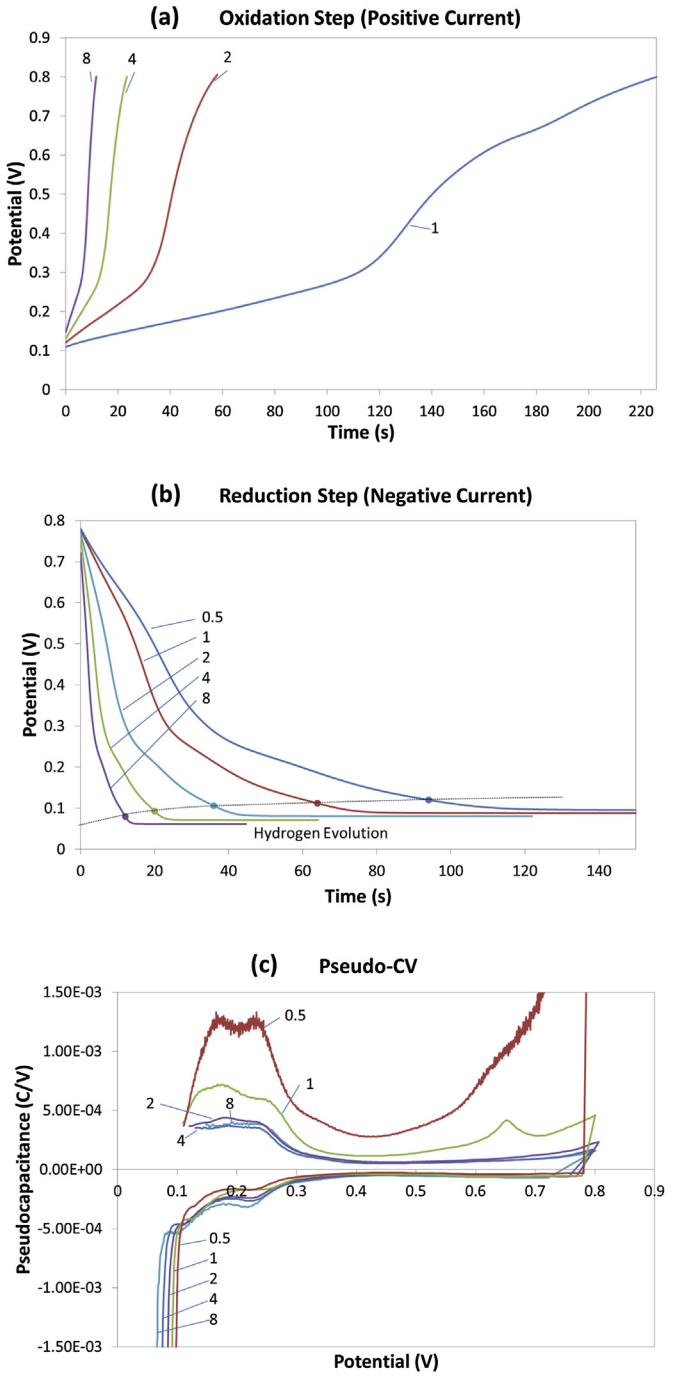

Fig. 2. (a) and (b) Galvanostatic measurements of (a) H oxidation and (b) H^+ reduction as a function of current density. (c) Galvanostatic data presented as pseudo-CV where $dQ/dV \approx i\Delta t/\Delta V$, with i = current density, t = time, V = potential. Current densities used are indicated in the figures in mA cm^{-2}.

Table 3
Galvanostatic ECSA determination using H adsorption.

Current density (mA cm^{-2})	ECSA from anodic current (m^2 g_{Pt}^{-1})	ECSA from cathodic current (m^2 g_{Pt}^{-1})
0.5	282	52
1	155	61
2	95	68
4	79	70
8	79	79

1, 2, 4 and 6 mA cm^{-2}. The results are plotted together with the previous data in Fig. 3. The experiments show good repeatability of the measurement, and a consistent trend of ECSA as a function of current density. Bearing in mind that the ECSA value obtained from CV data will also vary with scan rate, the key features for practical application of the technique are the repeatability of the galvanostatic measurements and the selection of an appropriate current density. At low current densities, the H oxidation measurements significantly overestimate and the H^+ reduction measurements underestimate the ECSA value due to the hydrogen crossover effect already discussed. However, both H oxidation and reduction measurements show relatively consistent ECSA values at intermediate current densities in the range 2–6 mA cm^{-2}.

3.1.3. Galvanostatic tests – CO stripping method

The onset of CO oxidation is well defined by a rapid decrease in the gradient dV/dt, as can be seen in the graph of potential against time in Fig. 4(a). The exact potential at which CO oxidation begins to occur appears to increase with increasing current density. This is similar to the behaviour observed in cyclic voltammetry, with an increasing sweep rate being analogous to increasing current density. The end of the CO oxidation plateau is less clearly defined, due to the more gradual upturn in the potential/time curve in Fig. 4(a). Therefore, in order to determine the charge passed for CO oxidation, a baseline was measured in the absence of CO, and the results were plotted in pseudo-CV form as described above. This is illustrated for the data obtained at 2 mA cm^{-2} in Fig. 4 (b). The resulting peak was then integrated to give the value of the charge passed to oxidise the CO.

The ECSA values obtained using the CO oxidation method at the five current densities used are summarised in Table 4. The results show a similar trend to the H oxidation data in that, without correcting for H_2 crossover, low current densities give an overestimate of the ECSA – indeed, a current density of 0.5 mA cm^{-2} could not be used because the cell potential did not rise to the cut-off point at all.

Both the CO stripping and H oxidation methods require the application of a positive current to the cell. If this is applied to a fuel cell stack, in which a distribution of ECSA values is present, the potential of individual cells in the stack will increase at different rates. It is therefore necessary to have a means of preventing the potential of any one cell from exceeding a safe limit, particularly in the case of CO oxidation. Although a method of selectively switching out individual cells using a relay board when each cell reaches a predefined voltage limit has been developed at NPL, this requires additional hardware and introduces undesirable complexity to the measurement. Accordingly, the H^+ reduction technique, in which potentials drift from high to low values, was selected for evaluation at stack level. Optimisation of the technique and attempts to minimise the effect of hydrogen crossover were carried out in the stack tests and will be discussed in Section 3.2.

3.2. Stack tests

3.2.1. Demonstration of technique at stack level

As mentioned in the previous section, whilst Lee et al. showed [7] that it is possible to separate out the individual contributions from H_{upd}, C_{dl} and H_2-crossover to the charge passed during the measurement, the objective of the present work was to develop a simple and easily applied test protocol to obtain a reliable estimate of ECSA for self-consistent comparison throughout stack lifetime. One significant limitation of the technique when applied to fuel cell stacks is the cell voltage data acquisition rate in the control hardware, which is typically limited to one measurement per second. This presents a challenge to more complex analysis of data. Rather than using the pseudo-CV to approximate the time from 400 mV to

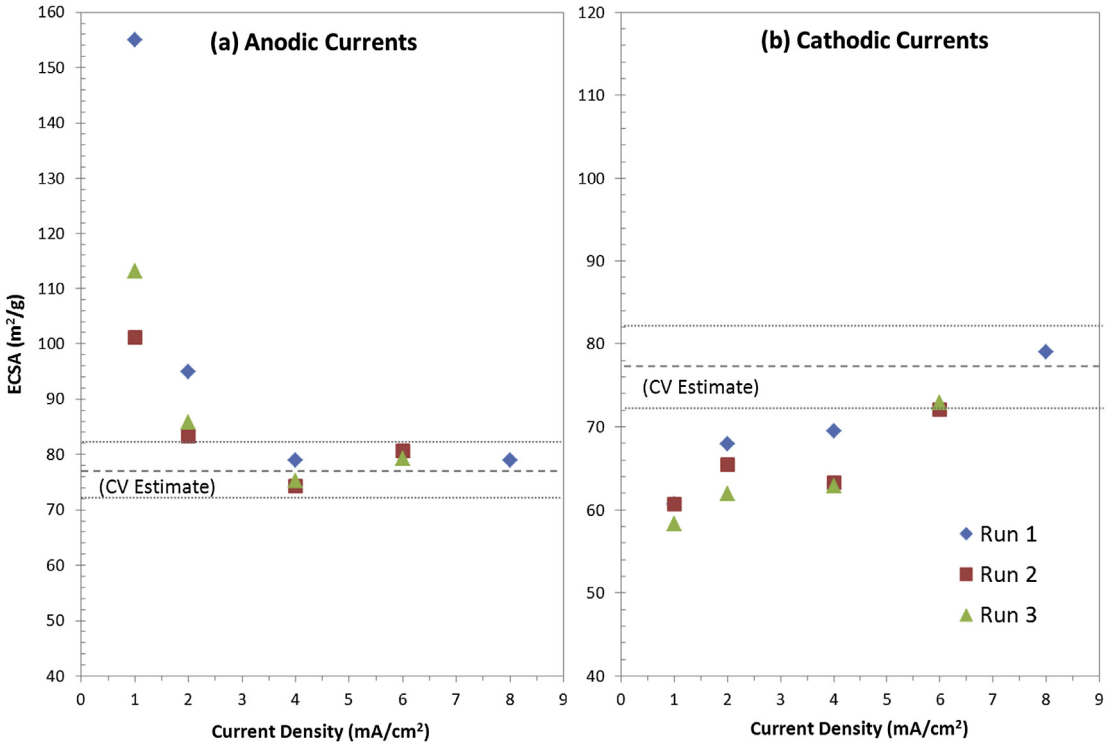

Fig. 3. ECSA estimated from the data in Fig. 3 (Run 1) and repeated at current densities of 1, 2, 4 and 6 mA cm^{-2} (Run 2 and Run 3).

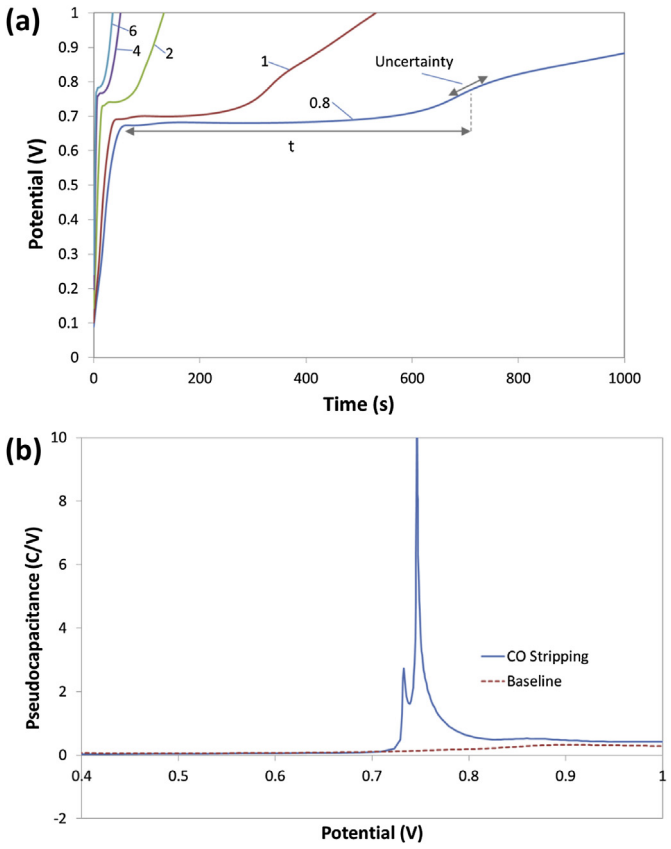

Fig. 4. CO stripping galvanostatic data. (a) Potential/time data; current densities are indicated on the figure in units of mA cm^{-2}. (b) Data plotted in pseudo-CV form together with baseline data in absence of CO for a current density of 2 mA cm^{-2}.

the onset of H_2 evolution on the reductive sweep (~0.1 V according to the data of Fig. 2b) the time elapsed between 400 mV and 100 mV was used to enable calculation of Q. The contribution of the double layer capacitance was found to make a small constant contribution to the measured charge and was disregarded for the purposes of this study, although its extraction would be straightforward for subsequent work. The primary focus was on identifying practical steps to minimise the contribution from H_2-crossover to the ECSA measurement in fuel cell stacks.

An example of the evolution of potential with time for all 18 cells in the stack during the galvanostatic measurement is shown in Fig. 5 and the corresponding distribution of ECSA values is summarised in Table 5. The technique is clearly applicable at stack level but a number of issues required further investigation. Firstly the measurement error due to H_2 crossover needed to be mitigated. To this end, the effect of using dilute H_2 on the anode was investigated. The second area of investigation was to establish the sensitivity of this technique to MEAs with different Pt loadings when built in a mixed stack, particularly due to potential neighbouring effects of MEAs of differing constructions. Thirdly, and perhaps of most concern, the measured ECSA value depends strongly on the applied current density. This is partly due to the fact that the inherent hydrogen crossover through PFSA membranes will lead to a reduction of the cathode voltage independent of any applied discharge current. Therefore, selection of a higher discharge current

Table 4
Galvanostatic ECSA determination using CO stripping.

Current density (mA cm^{-2})	ECSA (by area on dQ/dV vs V plot) (m^2 g_{Pt}^{-1})
0.8	265
1	95
2	77
4	57
6	63

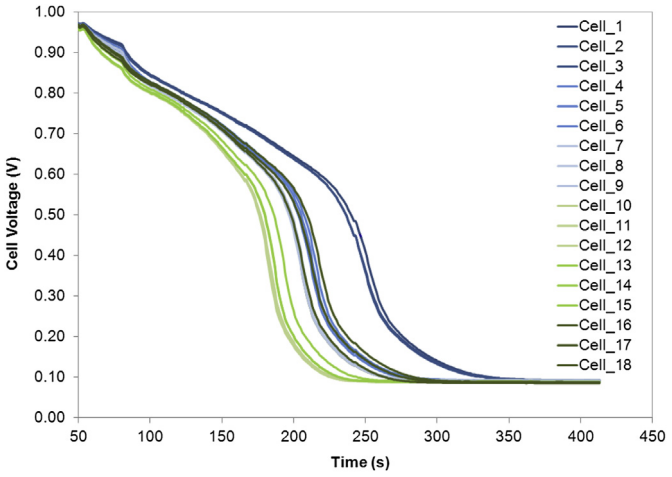

Fig. 5. Example discharge voltages from MEAs of Table 1 in an 18-cell stack; 10% H_2, 0.5 mA cm^{-2}. MEAs comprising Membrane 1 (blue) and Membrane 2 (green). (For interpretation of the references to color in this figure legend, the reader is referred to the web version of this article.)

would cause the voltage to drop at a sufficiently fast rate that the hydrogen crossover has negligible impact. However, this must be balanced against the loss of measurement accuracy due to the limited time resolution of voltage measurement on the test stand. Finally, as PFSA membranes age (e.g. via formation of pinholes or general thinning), hydrogen crossover through the membrane will increase and thus, the contribution of hydrogen crossover to the voltage discharge rate will also increase with time. This may lead to a possible underestimation of the cathode Pt area – an error which may increase over the MEA life. These issues are explored in the following sections.

3.2.2. Impact of anode hydrogen concentration

The impact of varying the anode H_2 concentration on the time taken for the cathode voltage to discharge is shown in Fig. 6(a). The data from just one cell from the stack are shown for clarity (Cell 2 Membrane 1, 0.4 mg cm^{-2} cathode). As discussed above, the use of hydrogen concentrations <10% was not practical on the test stand used. Clearly, higher H_2 concentrations lead to a reduction in the time required to fully discharge the cathode, as would be expected from the increased H_2 crossover which also contributes to decreasing the cathode voltage.

Table 5
Galvanostatic roughness factors of stack MEAs determined from a range of applied current densities; 10% H_2 (Build One). Discharge currents are negative currents.

Cell #	Roughness factor (cm^2_{Pt} $cm^{-2}_{electrode}$) applied current: 0.0 mA cm^{-2}	Roughness factor (cm^2_{Pt} $cm^{-2}_{electrode}$) applied current: 0.5 mA cm^{-2}	Roughness factor (cm^2_{Pt} $cm^{-2}_{electrode}$) applied current: 1.0 mA cm^{-2}
1	148	233	333
2	152	233	324
3	145	238	324
4	126	200	248
5	133	186	248
6	133	186	248
7	119	171	248
8	121	176	229
9	126	190	248
10	105	171	219
11	100	157	229
12	102	157	229
13	105	171	238
14	110	181	257
15	107	167	229
16	138	233	314
17	143	210	295
18	129	214	276

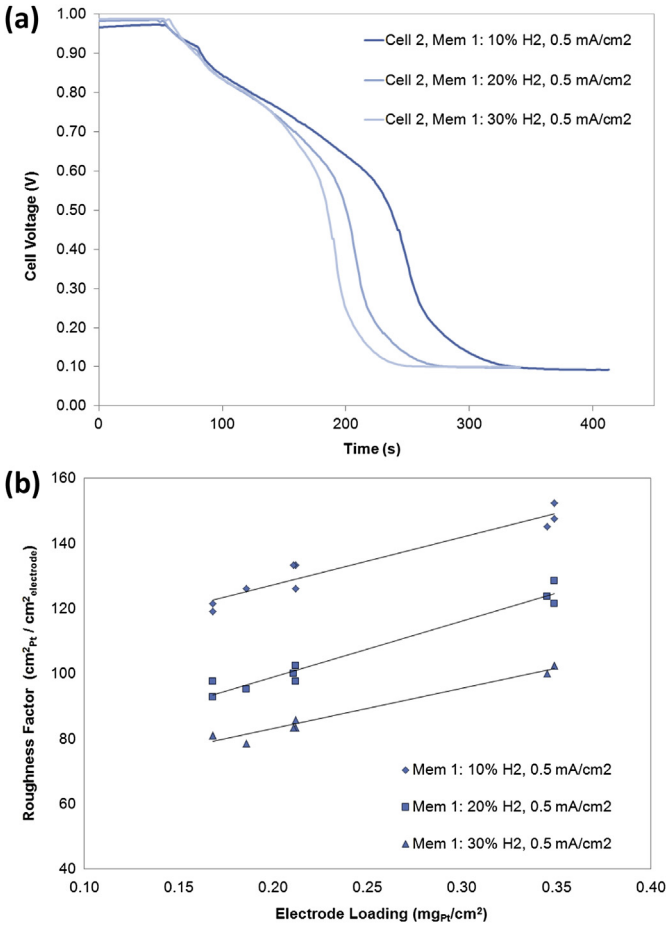

Fig. 6. (a) Effect of anode H_2 concentration on voltage discharge time, Cell 2. (b) Effect of anode H_2 concentration on current derived roughness factor.

Fig. 6(b) shows the calculated roughness factor (RF) determined from the raw data of the type shown in Fig. 6(a) from the entire sample set containing Membrane 1 (Cells 1–9) under a discharge current density of 0.5 mA cm^{-2}. As seen in Fig. 6(a), an increase in hydrogen concentration leads to a decrease in discharge time which results in a reduction in the calculated ECSA for all cells.

Fig. 7 compares the calculated RF for all three cathode loading variants with the two different membranes; data from the three different H_2 concentrations are shown on independent plots for clarity. The higher H_2 permeation rate of Membrane 2 leads to a lower apparent RF compared to Membrane 1. The offset of the measured data is fairly constant at all three H_2 concentrations that were used in this study, corresponding to ~20 s faster discharge time for Membrane 2 compared with Membrane 1. It is unknown whether this offset would be reduced by use of an even lower H_2 concentration, but clearly the H_2 crossover has a significant effect on the calculated ECSA, and since it is important to minimise this error it would be advisable to use the lowest H_2 concentration practicably possible – whilst still ensuring that the anode electrode can maintain a stable reference potential.

3.2.3. Sensitivity to electrode loading

The data of Fig. 6 have clearly shown that this galvanostatic technique is readily able to detect variations in cathode loading with no obvious indication that the position of the MEA within the

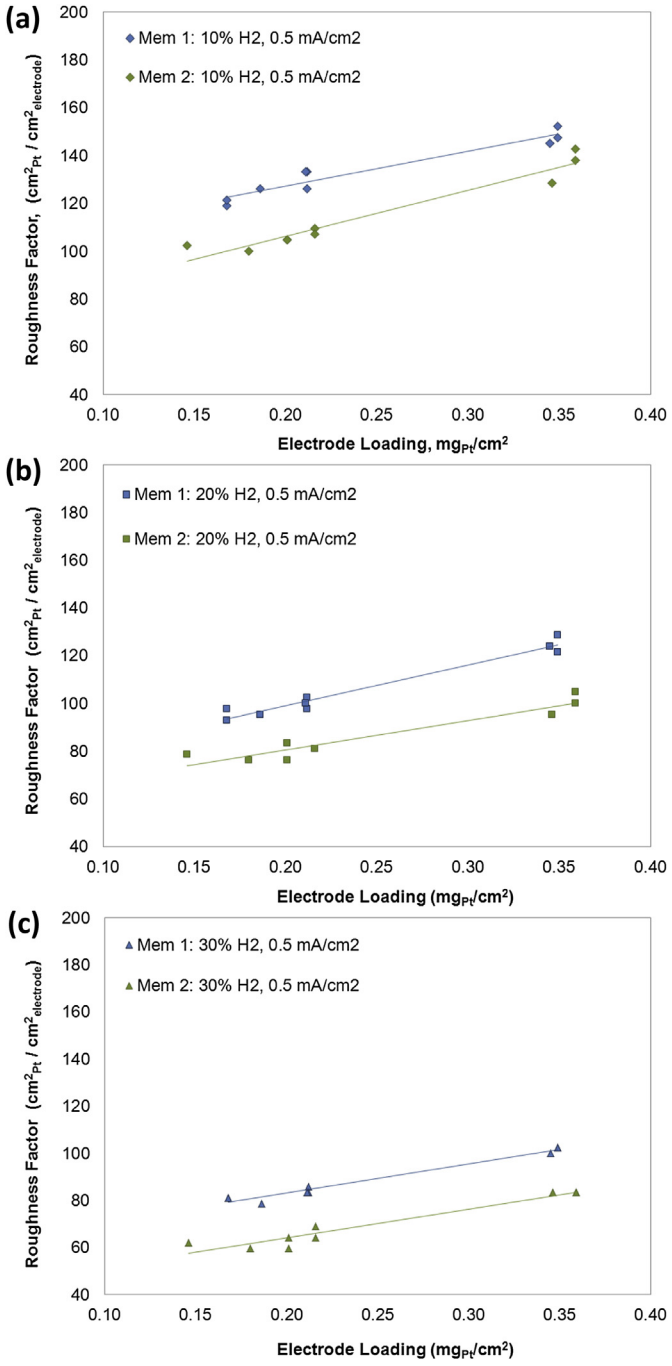

Fig. 7. Impact of H_2 concentration on calculated roughness factors from MEAs containing Membrane 1 (blue) and Membrane 2 (green). (For interpretation of the references to color in this figure legend, the reader is referred to the web version of this article.)

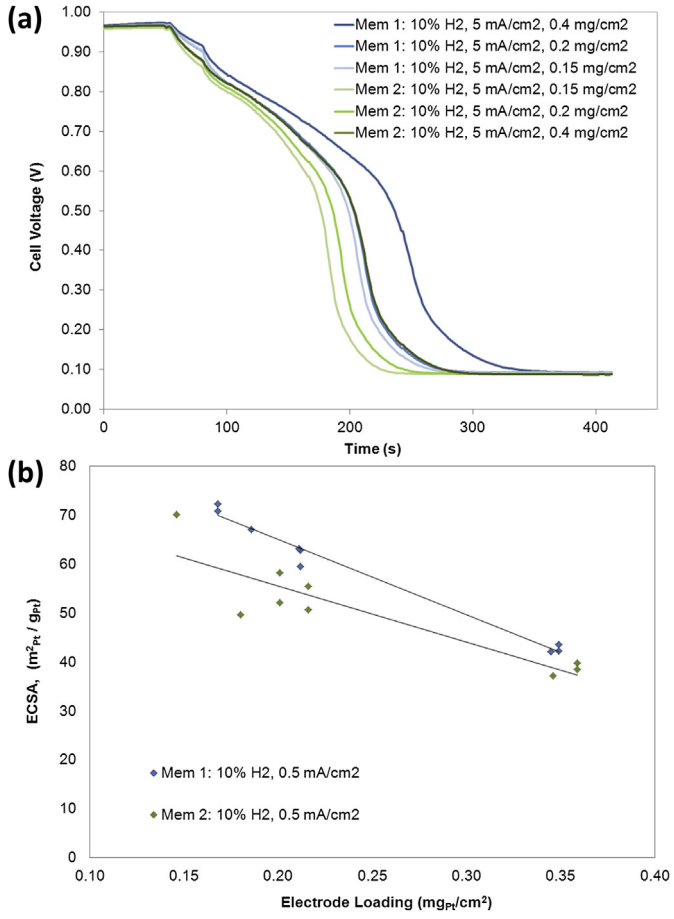

Fig. 8. (a) Variation in cathode discharge time as a function of cathode loading for each of the two membranes: 5% H_2, 5 mA cm^{-2}. (b) Variation in calculated ECSA as a function of electrode loading for all 18 cells in the stack; 10% H_2, 0.5 mA cm^{-2}.

stack has any bearing on the calculated ECSA (i.e. there are no obvious deviations from the linear trend). Furthermore, loading variations are detectable by calculation of the roughness factor, independent of the H_2 concentration employed. Under any one hydrogen concentration, the time taken to discharge the cathode layer is clearly dependent on the loading of the catalyst, as would be expected – this is illustrated by the raw data for cells 2, 5, 8, 11, 14 and 17 in Fig. 8(a) and for all 18 cells in Fig. 8(b).

Translating the discharge times from the raw voltage vs. time data, first to RF (the total Pt area per area of electrode), and then correcting for the actual electrode loadings to yield ECSA, should result in a normalised dataset for which the same metal area $m^2\ g_{Pt}^{-1}$ is reported for all electrodes given that the same catalyst was employed for each of the MEA variants. The Pt/C electrocatalyst used in this work has a gas phase CO metal area (i.e. measurement of the catalyst powder) of ~85 $m^2\ g^{-1}$. The metal area actually accessed in an operational MEA is known to be less than this, with 80–90% of the total area realised in an MEA [9], contingent upon an effective design of the electrocatalyst layer. Thus, the expected in-cell ECSA of the MEAs in this study is ~68–77 $m^2\ g_{Pt}^{-1}$. As will be reported, variation between the three cathode sets from this range is observed. This may, in part, be attributable to the fact that in order to keep all cathode variables the same, other than the loadings, the cathode structures are not optimised to take account of their thickness.

Fig. 8(b) shows the calculated ECSA values of all 18 cells in the stack measured under 10% H_2 and 0.5 mA cm^{-2} reverse current. There is a clear distribution in the calculated ECSA values which range from 42 to 72 $m^2\ g_{Pt}^{-1}$ (Membrane 1) and 37–70 $m^2\ g_{Pt}^{-1}$ (Membrane 2). Those metal areas calculated from the higher loaded electrocatalyst layers show the largest deviation from the expected 68–77 $m^2\ g_{Pt}^{-1}$. As shown in Fig. 8(a), the layers with the highest Pt loading (thicker layers) take the longest time to discharge and, thus, are more sensitive to the effects of hydrogen crossover (which, as already discussed, causes the cell voltage to drop at a faster rate than if driven by applied current alone). So, clearly H_2 permeation still has an adverse effect on the measurement despite the fact that only a low concentration was employed.

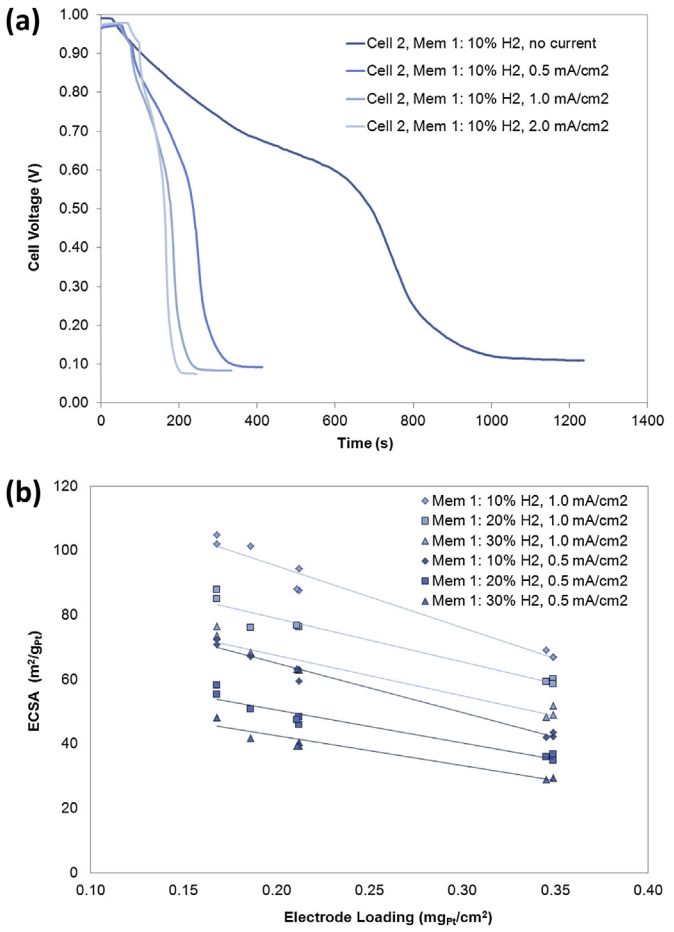

Fig. 9. (a) Effect of current density on voltage discharge time, Cell 2 (Membrane 1) (b) Calculated ECSA under reverse currents of (i) 0.5 mA cm^{-2} (ii) 1.0 mA cm^{-2} and varying anode H_2 concentrations for cells containing Membrane 1.

3.2.4. Sensitivity to applied current density

In order to more accurately determine ECSA across a range of MEA designs, loadings and membrane variants, the voltage discharge must be rapidly induced by the applied current such that any hydrogen crossover has a minimal effect on the discharge time and correspondingly, on the calculated ECSA values.

In the initial stages of stack testing, current densities of −0.5, −1.0 and −2.0 mA cm^{-2} were applied. Fig. 9(a) shows the impact of applied current density on the discharge time with a comparison against the case in which no current is applied (i.e. when only H_2 crossover is discharging the cathode electrode). The reduction in discharge time with increasing current density is evident and it is clear that use of a higher current density reduces the time window in which hydrogen crossover can influence the test results.

Fig. 9(b) shows the calculated ECSA values for all cells containing Membrane 1 under two different discharge current densities (−1.0 and −0.5 mA cm^{-2}) and under the range of hydrogen concentrations reported earlier. As predicted, the use of a higher current density leads to an increase in the calculated ECSA value because the discharge times are affected by hydrogen crossover to a lesser extent.

Now that the effects of hydrogen crossover are better understood, the preferred datasets for comparison are those obtained under the 10% H_2 concentration. Comparing this subset of data under −0.5 and −1.0 mA cm^{-2} current density (diamond shaped data points), it is observed that some of the calculated values fall into the expected band (68–77 m^2 g_{Pt}^{-1}) although others remain above or below the expected ECSA. A better fit may be achieved by use of some intermediate current density.

It is important to consider at this stage that for the stack measurements the voltage sampling interval was restricted to 1 s due to hardware limitations. This limited the measurement accuracy achievable at higher current densities (where the voltage falls more rapidly), and therefore required a balance to be found between minimising the error from H_2 crossover and maximising measurement resolution. To this end, one cell of each variant was removed from the stack and tested in equivalent single cell hardware using the conventional CV method. This provided ECSA data from which the calculated values of the stack galvanostatic method could be cross-compared. Both hydride and CO voltammetry were conducted, though the CO stripping method is preferentially used at JMFC owing to the greater resolution of the redox features of CO oxidation relative to H adsorption/desorption in an MEA. The results of this initial test suggested that the use of an intermediate current density, e.g. 0.75 mA cm^{-2}, would give an overall improvement in the agreement between the single cell and stack derived data. The fuel cell stack was therefore re-built with new MEAs, of an equivalent part design to those removed for assessment in the single cell, inserted at the same positions. The stack was reconditioned as before and stack 'cathode discharge' testing was completed under current densities of −0.5, −0.75 and −1.0 mA cm^{-2}. The new MEAs in positions 2, 5, 8, 11, 14 and 17 (i.e. one MEA of each variant) were again removed from the stack and the ECSA again determined in a single cell test under conventional potentiostatic conditions.

Table 6 compares the ECSA values for these six cells from (i) galvanostatic stack testing using H adsorption and (ii) conventional voltage-controlled single cell tests using CO stripping. Stack data collected under three current densities are shown using 10% H_2 on the anode; the values in brackets show the variation of the in-stack ECSA from the single cell CO ECSA data. For ease of comparison, these data are shown in graphical form (Fig. 10) with the error bars derived from an assumed error of ±1 s in the determination of the time taken for the cell potential to drop to 0.1 V.

With the use of the single cell data, it can be concluded that the new galvanostatic method does enable a reasonable estimation of the metal area of the cathode electrode, although there are some

Table 6
Build 2, comparison of stack galvanostatic ECSA vs. conventional single cell ECSA.

MEA	Mem.	Cell #	Loading mg_{Pt} cm^{-2}	Single CELL ECSA, m^2 g_{Pt}^{-1}		Stack ECSA, m^2 g_{Pt}^{-1} (variation from CO single cell) 10% H_2		
				H	CO	−0.5 mA cm^{-2}	−0.75 mA cm^{-2}	−1 mA cm^{-2}
1	Mem 1	2	0.345	50	54	47 (−7)	57 (3)	65 (11)
2	Mem 1	5	0.211	60	66	60 (−6)	74 (14)	84 (18)
3	Mem 1	8	0.163	73	79	77 (−2)	90 (13)	102 (23)
4	Mem 2	11	0.145	69	90	76 (−14)	89 (−1)	99 (9)
5	Mem 2	14	0.193	66	70	59 (−11)	72 (2)	76 (6)
6	Mem 2	17	0.346	44	52	41 (−11)	50 (2)	56 (4)

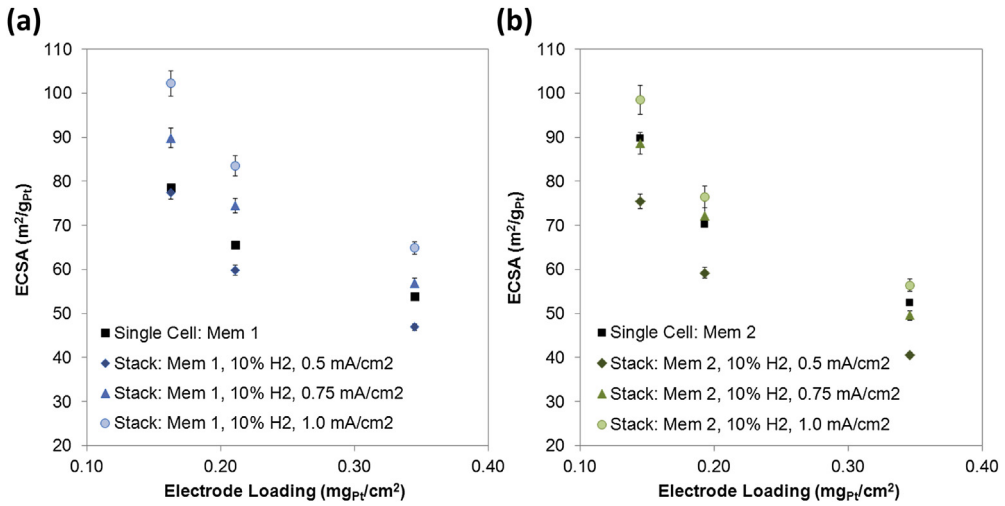

Fig. 10. Build 2; comparison of stack current-controlled ECSA determination with single cell CO ECSA (a) Membrane 1 (b) Membrane 2.

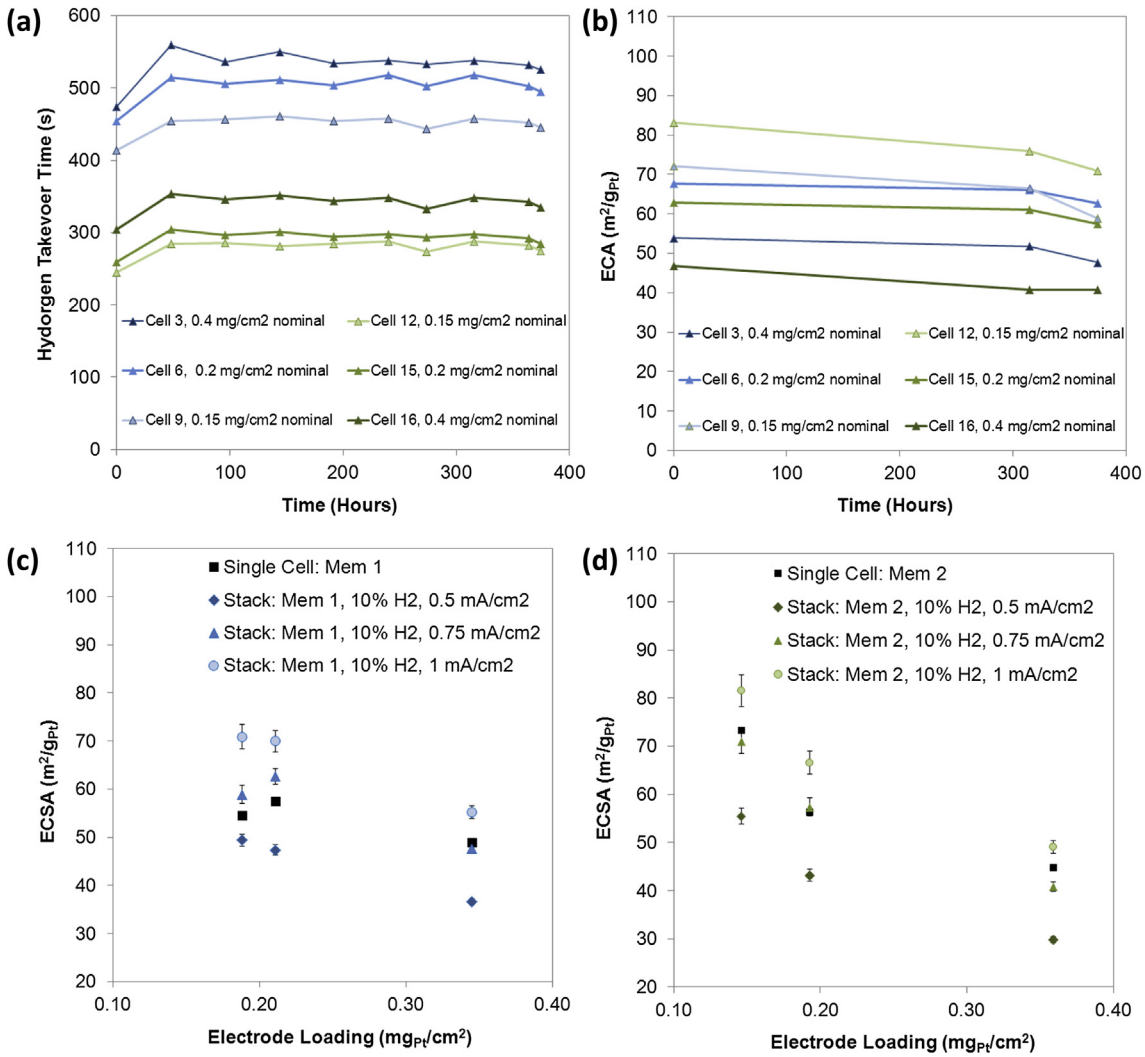

Fig. 11. Relating to Cells 3, 6, 9 (Membrane 1 – blue) and Cells 12, 15, 16 (Membrane 2 – green). (a) Hydrogen permeation of cells over ~400 h. (b) ECSA of cells derived from cathode discharge method, 10% H_2, 0.75 mA cm^{-2}. (c) Comparison of single cell CO ECSA and stack data for samples containing Membrane 1. (d) Comparison of single Cell CO ECSA and stack data for samples containing Membrane 2. (For interpretation of the references to color in this figure legend, the reader is referred to the web version of this article.)

sensitivities to MEA design. Although it could be argued that for Membrane 1 there is better agreement with single cell data for a current density of −0.5 mA cm^{-2}, particularly at the lower loadings, conventional PEMFC cathodes typically remain at 0.4 mg cm^{-2} with increasing tendency towards 0.2 mg cm^{-2}, in which case either −0.5 A cm^{-2} or −0.75 A cm^{-2} are acceptable selections of discharge current density. As discussed in Section 2.2.1, Membrane 2 was selected as a 'worst-case' scenario in terms of hydrogen crossover, with most advanced PEM membranes exhibiting gas crossover properties equivalent to or better than Membrane 1. In such cases, particularly considering the increased accuracy of data obtained from use of a lower current density, a more appropriate *general* selection of current density would be −0.75 mA cm^{-2}. For a given test stand, the optimum current density will depend on the capability for supplying low hydrogen concentrations to the anode and on the cell voltage sampling rate.

3.2.5. Effect of membrane aging

A final concern outlined at the start of Section 3 was the impact of membrane aging on the apparent ECSA. Specifically, as membranes degrade and thin, the hydrogen crossover increases; the impact of crossover on the rate of cathode discharge has already been demonstrated. To complete this validation study, the MEAs of the stack were aged under OCV conditions (see Section 2.2.3) with the intent of aging the membrane whilst monitoring any change in the cathode discharge response and finally, validating the ECSA post aging in single cell experiments. For this work new MEAs were added to the stack to replace those samples removed under the earlier single cell study (Fig. 10) such that the stack remained at 18 cells.

Fig. 11(a) shows the hydrogen permeation rate for Cells 3, 6, 9 (Membrane 1) and Cells 12, 15, 16 (Membrane 2). This test is routinely employed to assess the health of the membrane during stack testing, and the method is similar to the cathode discharge work reported here although without the application of load – see Fig. 9, "no current" data. As has been made apparent in the course of this paper, the design of the cathode electrode has a significant effect on the cathode discharge. As demonstrated in Fig. 11(a) in which the three datasets from Membrane 1 and separately Membrane 2 should be compared, thinner cathode electrodes discharge more quickly than thicker electrodes. Thus, the hydrogen permeation test (i.e. the absolute time taken for the cell voltage to fall) is not entirely representative of membrane health and the data must be assessed by a *change* in hydrogen permeation rate with time. As Fig. 11(a) shows, there was in fact little change in the hydrogen permeation rate of the membrane over the OCV testing for the first 300 h, with perhaps a small decrease in permeation time after this. After 300 h, the stack ECSA measurements suggested that the cathode metal area had decreased (Fig. 11(b)) raising the expected question as to whether this was a genuine degradation of the cathode electrode (N.B. OCV testing is not typically considered damaging to electrocatalyst layers) or an artefact of small changes in membrane health. Fig. 11(c) and (d) compare the stack ECSA data under the range of current densities used herein vs. the CO ECSA values on removal of these six cells from the stack and assessment in the single cell hardware. Again, the data obtained under the −0.75 mA cm^{-2} current density compared well with those from the single cell. Notably, by comparison with the ECSA of those samples assessed prior to any aging work (i.e. data of Fig. 10), the data do indeed suggest that OCV testing causes degradation of the cathode electrode, with the electrodes losing on average 8 m^2 g^{-1} Pt over the 400 h test. In the case herein, it is not known whether this is attributable to Pt agglomeration or catalytic isolation of Pt either via carbon loss or degradation of the cathode ionomer (Gittleman et al. have recently noted that there is little conclusive evidence for the latter [10]). Extended OCV testing was not continued beyond that reported here. As it is anticipated that membrane thinning will impact the calculated ECSA values, it is recommended that this galvanostatic method is used in conjunction with other stack lifetime diagnostics (e.g. hydrogen permeation, short testing) which should indicate when membrane health becomes problematic.

4. Conclusions

- We have demonstrated for the first time the practical application of a novel galvanostatic technique for in situ measurement of ECSA in each cell of a PEMFC stack. This technique is straightforward to implement and provides an invaluable tool for state of health monitoring during fuel cell durability tests.
- The H adsorption (cathodic current) method shows most promise for application in fuel cell stacks as there is no risk of damage to individual cells at positive potentials. Good agreement was obtained with ECSA values determined using conventional single cell voltammetry across a range of MEA designs.
- The technique is readily able to discriminate between cathodes with different electrode loadings and is insensitive to the position of the MEAs within the stack, i.e. there are no adverse neighbouring effects.
- The effect of hydrogen crossover on the measurement can be minimised by the use of a low hydrogen concentration on the anode and an appropriate selection of current density. As such, there is some requirement to (i) know the initial ECSA of the cathode electrode to set the conditions for the experiment or (ii) accept some error in the initial ECSA. In either case, the technique can be successfully employed to monitor Pt area with time.

Acknowledgements

This work was supported by the UK National Measurement System and the Technology Strategy Board under contract number BH064B. The authors would like to thank Carlos Prieto, Wayne Turner and Barry Wade of JMFC for their significant efforts in the translation and further development of this technique from NPL. Their inputs into both experimental work and data reduction tasks are gratefully acknowledged.

References

[1] J. Wu, X.Z. Yuan, J.J. Martin, H. Wang, J. Zhang, J. Shen, S. Wu, W. Merida, Journal of Power Sources 184 (2008) 104.
[2] A.M. Chaparro, A.J. Martín, M.A. Folgado, B. Gallardo, L. Daza, International Journal of Hydrogen Energy 34 (2009) 4838.
[3] R.W. Lindstrom, K. Kortsdottir, M. Wesselmark, A. Oyarce, C. Lagergren, G. Lindbergh, Journal of the Electrochemical Society 157 (2010) B1795.
[4] B.E. Conway, G. Jerkiewicz, Electrochimica Acta 45 (2000) 4075.
[5] T. Biegler, D. Rand, Journal of Electroanalytical Chemistry 29 (1971) 269.
[6] S. Wasterlain, D. Candusso, F. Harel, D. Hissel, X. François, Journal of Power Sources 196 (2011) 5325.
[7] K.-S. Lee, B.-S. Lee, S.J. Yoo, S.-K. Kim, S.J. Hwang, H.-J. Kim, E. Cho, D. Henkensmeier, J.W. Yun, S.W. Nam, T.-H. Lim, J.H. Jang, International Journal of Hydrogen Energy 37 (2012) 5891.
[8] D.A. Stevens, J.R. Dahn, Journal of The Electrochemical Society 150 (2003) A770.
[9] H.A. Gasteiger, S.S. Kocha, B. Sompalli, F.T. Wagner, Applied Catalysis B: Environmental 56 (2005) 9.
[10] C.S. Gittleman, F.D. Coms, Y.-H. Lai, in: M.M. Mench, E.C. Kumbur, T.N. Veziroglu (Eds.), Polymer Electrolyte Fuel Cell Degradation, Academic Press, 2012, p. 26.